PNAS
www.pnas.org

Supplementary Information for
Soluble α-synuclein/antibody complexes activate the NLRP3 inflammasome in hiPSC-derived microglia.

Dorit Trudler,[1,3] Kristopher L. Nazor,[4] Yvonne S. Eisele,[5,6], Titas Grabauskas,[1] Nima Dolatabadi,[1,3] James Parker,[3] Abdullah Sultan,[3] Zhenyu Zhong,[7,8] Marshall S. Goodwin,[9] Yona Levites,[9] Todd E. Golde,[9] Jeffery W. Kelly,[1,5] Michael R. Sierks,[10] Nicholas J. Schork,[11,12] Michael Karin,[7] Rajesh Ambasudhan,[1,3†] and Stuart A. Lipton[1-3,13†*].

* Correspondence regarding the manuscript should be addressed to S.A.L. and R.A.
Email: slipton@scripps.edu, rajesh@scintillon.org

This PDF file includes:

Supplementary text (Extended Materials and Methods)
Figures S1 to S4
Tables S1 to S2
Legends for Datasets S1 to S3

Other supplementary materials for this manuscript include the following:

Datasets S1 to S3

Supplementary Information Text

Extended Materials and Methods

hiPSC Cultures. The use of human cells was approved by the institutional review boards of the Scintillon Institute and The Scripps Research Institute (TSRI). hiPSCs were generated from normal human fibroblasts (Hs27, ATCC CRL-1634 and Coriell, GM02036) by using an integration-free reprogramming method (1), which uses three episomal vectors that collectively encode OCT3/4, SOX2, KLF4, L-MYC, LYN28, and p53-shRNA. Details of the hiPSC characterization are described elsewhere (2). hiPSCs were routinely cultured and maintained in our laboratory using a protocol described previously (3) with some modifications. Briefly, pluripotent cells were plated on Matrigel coated plates (Corning, #354248) and cultured using mTeSR1 (STEMCELL Technologies, #05850) changed daily. The colonies were manually passaged weekly, using StemPro™ EZPassage™ Disposable Stem Cell Passaging Tool (Thermo-Fisher Scientific, #23181010).

hiMG Differentiation. Detailed information concerning media composition, growth factors and catalog numbers appear in **Table S1**. When hiPSCs reached 80% confluence, they were lightly passaged using StemPro™ EZPassage™ Disposable Stem Cell Passaging Tool to form small size clumps. Aggregates were allowed to settle, and the medium changed to hiMG induction medium [StemPro34 containing GlutaMAX™ (2 mM), L-ascorbic acid 2-phospate (64 µg/ml) and MTG (0.46 mM), abbreviated as MGIM] supplemented with BMP4 (10 ng/ml) and ROCK inhibitor Y27632 (10 µM). Each well of aggregates was transferred to a well of an ultra-low attachment plate (Corning), in 5% O_2, 5% CO_2. The next day (day 1), the same volume of MGIM, supplemented with BMP4 (10 ng/ml), ROCK inhibitor Y27632 (1 µM), and bFGF (10 ng/ml), was added. On day 4, embryoid bodies (EBs) were collected and the medium was changed to MGIM, supplemented with bFGF (1 ng/ml), VEGF (10 ng/ml), IL-6 (10 ng/ml), IL-3 (40 ng/ml) and SCF (100 ng/ml), and returned to low oxygen conditions for 4 more days. On day 8, the medium was changed to MGIM supplemented with VEGF (10 ng/ml), IL-6 (10 ng/ml), IL-3 (40 ng/ml), TPO (50 ng/ml) and SCF (100 ng/ml). At this point, the plate was transferred to normoxic conditions with 21% O_2. On day 11, the same volume of medium was added to each well. On day 15, EBs were collected, and the medium was changed to hiMG differentiation medium [(Iscove's Modified Dulbecco's Medium (IMDM) containing 1% N2, 0.5% BSA, 0.2% AlbuMAX®, L-ascorbic acid 2-phospate (64 µg/ml) and MTG (0.46 mM)], supplemented with IL-34 (100 ng/ml) and GM-CSF (10 ng/ml). This medium composition was used from this point forward. At this stage cells start to attach to the low attachment plate. On day 18, an equal volume of medium was added, and enhanced cell attachment was evident. By day 21, hiMGs were fully attached and were then

dissociated for 2 min with enzyme-free dissociation buffer (Gibco, #13151014). The cells were counted and plated at a density of $4x10^4/cm^2$ on regular tissue culture plates for biological experiments, or $1x10^4/cm^2$ on glass coverslips (acid-washed) for imaging experiments. All experiments were carried out 2-5 days after re-plating; 16 h before the experiment, the medium was changed to IMDM without supplements. For gene expression analysis at various time points of the differentiation, a small sample was removed. The initial differentiation procedure was perfected successfully on at least 6 different lines, and all subsequent experiments were performed on at least 2 different hiPSC lines (male and female) using at least 3 independent differentiations.

Abbreviations: Monothioglycerol (MTG); bone morphogenic protein 4 (BMP4); basic fibroblast growth factor (bFGF); vascular endothelial growth factor (VEGF); interleukin (IL); Stem cell factor (SCF); thrombopoietin (TPO); granulocyte-macrophage colony stimulating factor (GM-CSF).

Primary Astrocytes. Primary astroglial cultures were prepared as previously described (4). Mice used for astrocyte cultures were housed and maintained in the animal facility at the Scintillon Institute or The Scripps Research Institute, and all experiments complied with protocols approved by the Institute Animal Care Committee. The brains from 1- to 2-day-old C57BL/6 mouse pups were rapidly harvested, and the meninges were removed. Brains were dissociated using mechanical means (pipettes and scissors) and enzymatic dissociation (0.25% trypsin for 30 min at 37 °C). The cell suspension was then filtered through a 70-µm cell strainer and cultured in DMEM:F12 medium supplemented with 10% fetal bovine serum, 100 U/ml penicillin, and 0.1 mg/ml streptomycin. Two weeks after initial isolation, cells were dissociated with Accutase (STEMCELL Technologies, #07920), and the suspension was seeded onto glass coverslips coated with 20 $\mu g/cm^2$ poly-L-ornithine (Sigma-Aldrich, #P4638) and 2 $\mu g/cm^2$ laminin (Trevigen, #3400-010-01) and 2 $\mu g/cm^2$ fibronectin (Trevigen, #3420-001-01), at a density of 25,000 cells/cm^2.

hiPSC-Derived A9-Type DA Neurons. Differentiation of hiPSCs into A9-type DA neurons was performed as described previously (5, 6). Floor-plate induction was carried out using medium containing knockout serum replacement (KSR), LDN193189 (100 nM), SB431542 (10 µM), sonic hedgehog (SHH) C25II (100 ng/ml), purmorphamine (2 µM), fibroblast growth factor 8 (FGF8; 100 ng/ml), and CHIR99021 (3 µM). On day 5 of differentiation, KSR medium was incrementally shifted to N2 medium (25%, 50%, 75%) every 2 days. On day 11, the medium was changed to Neurobasal/B27/GlutaMAX supplemented with CHIR9902, brain derived neurotrophic factor (BDNF; 20 ng/ml), ascorbic acid (0.2 mM), glial derived neurotrophic factor (GDNF; 20 ng/ml), transforming growth factor β3 (TGFβ3; 1 ng/ml), dibutyryl cAMP (db cAMP; 0.5 mM), and DAPT

(10 μM). From day 13 onward, CHIR99021 was removed, and cells were cultured until day 20. Day 20 cells were dissociated using Accutase and re-plated under high cell density in DA medium on dishes pre-coated with 0.2% polyethylenimine (PEI) and poly-D-ornithine (15 μg/ml)/laminin (1 μg/ml)/fibronectin (2 μg/ml). Conditioned medium (CM) was collected after 12-13 days of differentiation.

Microglia-Astrocyte-Neuron Co-Cultures. For co-culture experiments, neurons were re-plated on a bed of mouse astrocytes at a 2:1 ratio for 4 days, and then microglial cells were added (final cell ratio was DA neurons:astrocytes:hiMG of 4:2:1). The cells were cultured in DA medium supplemented with IL-34 (100 ng/ml), GM-CSF (10 ng/ml), and 0.5% heat-inactivated fetal bovine serum (HI-FBS).

Microglial Engraftment. Triple transgenic NSG-SGM3 (NSGS) mice expressing human IL-3, GM-CSF (granulocyte-macrophage colony-stimulating factor) and SCF (stem cell factor) were purchased from Jackson (#013062), and approved for use by the Institutional Animal Care and Use Committee (IACUC) at The Scripps Research Institute. The mice were previously characterized to support human myeloid cell engraftment (7). For the αSyn pre-treatment experiments, hiMG were incubated with oligomeric αSyn for 6 hours prior to washing and dissociating. hiMG were collected at day 24 of differentiation and suspended in PBS. The cells were combined with either oligomeric αSyn (final dose of 0.5 μg/mouse), or with oligomeric αSyn (final dose of 0.5 μg/mouse) plus anti-αSyn Ab scFv (final dose of 100 ng/mouse) immediately prior to injection. The cells were injected stereotactically into 4-week-old female mice because they show better engraftment than males (8). Mice were anesthetized with isoflurane and immobilized in a stereotactic apparatus. An injection of 200,000 cells in a volume of 2 μl of PBS was delivered over a 10-minute period into the ventricle using the following coordinates from the bregma: mediolateral (ML) -1 mm; anteroposterior (AP) -0.3 mm; dorsoventricular (DV) 2.4 mm. Mice were administered two analgesic injections, immediately after the injection and 24 h later. Brains were collected 14 days post injection. For this purpose, the mice were anesthetized with an overdose of isoflurane. The brains were then removed, placed into 4% PFA overnight for fixation, and sunk in 30% sucrose in PBS prior to freezing. Cryostat sections were cut at a thickness of 20 μm.

Primary Mouse Microglia. Primary microglial cultures were prepared as previously described (9). Mice used to harvest microglia were housed and maintained in the animal facility at The Scripps Research Institute, and all experiments complied with protocols approved by the

Institutional Animal Care Committee. The brains from 1- to 2-day-old C57BL/6 mouse pups were rapidly harvested, and the meninges were removed. Brains were dissociated using mechanical means (pipettes and scissors) and enzymatic dissociation (0.25% trypsin for 30 min at 37 °C). The cell suspension was then filtered through a 70-µm cell strainer and cultured in DMEM:F12 medium (Thermo-Fisher, #10565042) supplemented with 10% fetal bovine serum (Thermo-Fisher Scientific, #10439024), 100 U/ml penicillin, and 0.1 mg/mL streptomycin (Thermo-Fisher Scientific, #15140122), and plated on glass coverslips coated with 20 µg/cm^2 poly-L-ornithine (Sigma-Aldrich, #P4638) and 2 µg/cm^2 laminin (Trevigen, #3400-010-01). At 18 days after initial isolation, astrocytes were removed by mild trypsinization with 0.05% trypsin (Thermo-Fisher Scientific, #25200056) for 2 hours (9), and adherent microglial cells remained for two more days prior to experimentation.

Preparation of Humanized scFv Against αSyn. scFv has been previously generated and characterized (10). scFv was expressed and isolated as previously described with some modifications (11). Briefly, soluble scFv was produced by expressing recovered phagemid samples in the non-suppressor *E.coli* strain HB2151. scFv production was induced by addition of 1 mM isopropyl-β-D-thiogalactopyranoside (IPTG, Sigma) and incubated overnight at 30 °C. The supernatant and periplasmic fractions were combined and applied to HisPur Cobalt Resin (Thermo-Fisher Scientific, #90091), eluted with 10−25 mM imidazole and buffer exchanged to PBS (Thermo-Fisher Scientific, #90011). The eluates were quantified with a Pierce™ BCA Protein Assay Kit (Thermo-Fisher Scientific, #23225).

Preparation of Humanized Antibody Against Aβ. The scFv against panAβ was previously generated and characterized (12). Here, anti-pan Aβ scFv was fused to human Fc1 to create a minibody scFv-Fc. Minibodies were expressed in HEK293 cells for 48 h and isolated from the conditioned medium using HisPur Cobalt Resin (Thermo-Fisher Scientific, # PI90092), eluted with 10−25 mM imidazole, and buffer exchanged to PBS (Thermo-Fisher Scientific, # PI87773). The eluates were quantified with a Pierce™ BCA Protein Assay Kit (Thermo-Fisher Scientific, #23225), and analyzed for purity on a gel with an InVision™ His-Tag In-Gel Staining Kit (Thermo-Fisher Scientific, # LC6033).

α-Synuclein Preparations. α-Synuclein was prepared as previously described (13). In brief, Endotoxin-free recombinant human α-synuclein protein was purchased commercially (Anaspec, #AS-55555-1000)**.** The protein was dissolved in HPLC-grade water (Sigma-Aldrich, #270733) at a concentration of 200 µM. Monomers were immediately aliquoted and frozen at -80 °C. For

oligomerization, samples were placed in a thermomixer and shaken continuously at 1,400 rpm for 6 days at 37°C, centrifuged at 1,000xg, and the pellet aliquoted and frozen at -80 ºC. For time-point analysis, aliquots were collected from the same oligomerization preparation at different times, and frozen at -80 ºC . For injections, oligomers were sonicated for 15 min, based on the previously described pre-formed fibril protocol (14).

Oligomeric Aβ Preparation. Amyloid-β peptide (Aβ, Anaspec, #AS-20276) was prepared as previously described (2). Briefly, Aβ was suspended in hexafluoroisopropanol to a concentration of 1 mM in and incubated overnight at room temperature, and solvent was evaporated in a SpeedVac. Peptide was resuspended in dry DMSO to a final stock concentration of 5 mM and diluted 10-fold in MEM (GIBCO) and was then incubated at 4 °C for ≥24 h. The percentage of soluble oligomers (that were used for experiments) is 15%.

α-Synuclein Characterization by Dynamic Light Scattering (DLS). Samples were removed from storage at -80 ºC, thawed gradually on ice, and gently resuspended. A 10 µl aliquot was then removed and monitored at room temperature (RT) on a Wyatt DynaPro NanoStar DLS instrument in disposable microcuvettes (Wyatt, #162960) with a 5 s acquisition time, 3x10 acquisitions per sample. Dynamics software Version 7.6.1 (Wyatt) was used for data analysis. Aggregates of various sizes were subdivided into three categories based on their apparent hydrodynamic diameter (D), as follows: D 10-200 nm; D 200-2,000 nm; D > 2,000. GraphPad Prism 7.04 was used for statistical analysis.

Pro-inflammatory and Inflammasome Activation. For the lipopolysaccharide (LPS) experiments, 16 h before the experiment the cell medium was changed to IMDM (no supplements added). hiMG were stimulated with ultrapure LPS (Invivogen, #tlrl-3pelps) at a concentration of 1, 10, 100 ng/ml in IMDM for 4 h. Cell medium was collected and analyzed by ELISA. Cells were lysed and analyzed by qRT-PCR. For flow cytometry experiments, cells were stimulated with 200 ng/ml LPS for 4 h, then dissociated and analyzed.

For inflammasome induction, 16 h before the experiment the cell medium was changed to IMDM (no supplements added). hiMG were stimulated with ultrapure LPS at a concentration of 200 ng/ml in IMDM for 4h. Without changing the medium, NLRP3 agonists were added: 30-min stimulation with 4 mM ATP (Sigma-Aldrich**,** #A6559); 30-min stimulation with 10 µM nigericin (Invivogen, #tlrl-nig); 4-h stimulation with 400 µg/ml alum (Thermo-Fisher Scientific, #77161).

To test αSyn stimulation of the inflammasome, αSyn monomers or oligomers were initially pre-incubated with 1 µg/ml polymyxin B sulfate (Sigma-Aldrich, #P4932) for 15 min to

prevent TLR activation from possible endotoxin contamination, and then added to cells at a concentration of 1 µM for 6 h. For dose-response experiments, cells were exposed to oligomeric αSyn at different concentrations for 6 h.

To block NLRP3 inflammasome activation, siRNA (see below) or MCC950 was used. MCC950 (CAS 256373-96-3; Sigma-Aldrich or #5.38120 EMD MILLIPORE) was added at a concentration of 1 µg/ml simultaneous to αSyn exposure.

For the TLR neutralizing antibody experiments, hiMG were exposed to anti-hTLR2-IgA2 (Invivogen, #maba2-htlr2) or human IgA2 subclass control (Invivogen, #maba2-ctrl), and to anti-hTLR4-IgG1 (Invivogen, #mabg-htlr4) or IgG1 subclass control (Invivogen, #mabg1-ctrlm). All antibodies were incubated at a concentration of 25 µg/ml for 1 h and then αSyn was added for 6 h. To block TLR2 activity, TLR2-IN-C29 (Biovision, # B2121) was used at a concentration of 10 µM simultaneous to αSyn exposure.

For experiments to assess the effect of anti-αSyn antibody/αSyn complexes, conditioned medium (CM) or recombinant αSyn oligomers were incubated with 2.5 µg/ml antibody for 1 h prior to culturing hiMG in the CM for 16 h. We used humanized scFv against αSyn or human IgG1-Fc as a control (Thermo-Fisher, #10702HNAH250 or Abcam, #ab90285). For mouse microglial experiments, we used rabbit anti-αSyn antibody (Abcam, #ab138501) or rabbit IgG isotype control (Abcam, #ab172730), mouse anti-αSyn antibody (BD Biosciences, #610787) or mouse IgG1 κ isotype control (BD Biosciences, #554121), goat anti-αSyn antibody (Abcam, #ab2080) or goat IgG isotype control (Abcam, #ab37373), and sheep anti-αSyn antibody (Abcam, #ab6162) or sheep IgG isotype control (Abcam, #ab37385).

Immunodepletion of αSyn. Conditioned medium from WT and αSyn(A53T) hiPSC-derived dopaminergic A9-type neurons was incubated with 5 µg/ml rabbit anti-αSyn antibody (Abcam, #ab138501) or rabbit IgG isotype control (Abcam, #ab172730). The medium was then incubated with Pierce Protein A/G Magnetic Beads (Thermo-Fisher Scientific, #88802), according to the manufacturer's instructions. Briefly, 500 µl of sample were incubated with 25 µl of washed beads for 1 h at room temperature, and then collected with a magnet. The depletion was evaluated by ELISA (see below), and the CM was used for microglial-exposure experiments.

siRNA Targeting the NLRP3 Inflammasome. hiMG were transfected with siRNA particles designed to target NLRP3 (Life Technologies, #4392420; ID: s534396) or with a control siRNA (Life Technologies, #4390843) at a concentration of 50 nmol/ml. Vehicle contained transfection reagent only (Lipofectamine RNAiMAX Transfection Reagent [Life Technologies, #13778075]), used according to the manufacturer's instructions. Briefly, hiMG were plated in a 12-well or 96-

well plate at a concentration of $4x10^4/cm^2$. The next day, siRNA and transfection reagent were added; 48 h later, cells were washed and activated with oligomeric/aggregated αSyn for 6 h. Knockdown of NLRP3 expression was confirmed by western blot. Cytokine secretion was assessed at the end of the experiment by ELISA.

Immunoblots. Cells were lysed with cell lysis buffer (Cell Signaling Technologies, #9803) supplemented with protease inhibitor cocktail (Roche, #04693159001) and 10 µM SDS. Protein concentrations were determined using Pierce™ BCA Protein Assay Kit (Thermo-Fisher Scientific, #23225). Polyacrylamide gels (Novex, 8-12%) were used for protein separation prior to transfer onto nitrocellulose membrane, blockade with blocking buffer (Li-Cor) for 1h, washing with TBST, and reaction overnight at 4 ˚C with rabbit anti-NLRP3 (1:1,000; Abcam, #ab210491) and mouse anti-GAPDH (1:10,000; Sigma-Aldrich, #CB1001 EMD MILLIPORE). Membranes were then reacted with goat anti-rabbit or goat anti-mouse infrared (IR) dye-conjugated secondary antibody (Li-Cor antibody) for 1h at room temperature. The membrane was scanned using an Odyssey® scanner, quantified using Fiji software (15), and analyzed with Prism 7.04 software (GraphPad).

Enzyme Linked Immunosorbent Assay (ELISA). Quantitative ELISA for human IL-1β, IL-6 and TNF were performed using paired antibodies and recombinant cytokines obtained from eBioscence following the manufacturer's recommendations. ELISA for caspase 1/ICE was performed using a Quantikine ELISA Kit (R&D systems, #DCA100) according to the manufacturer's instructions. ELISAs were quantified with a SpectraMax plate reader (Molecular Devices). ELISA for human αSyn was performed using a Legend MAX ELISA kit (BioLegend, #844101) according to the manufacturer's instructions, and quantified using a Luminoskan Ascent Microplate Luminometer (Thermo-Fisher Scientific). All ELISA measurements were analyzed with Prism 7.04 software (GraphPad).

Detection of Mitochondrial Reactive Oxygen Species (ROS) with MitoSOX. Mitochondrial ROS was measured using MitoSOX™ red mitochondrial superoxide indicator (Thermo-Fisher Scientific, #M36008) according to the manufacturer with some modifications. Briefly, cells were loaded with 2.5 µM dye in medium for 15 min at 37 ºC. Cells were washed with PBS twice, and then fixed with 4% PFA. The cells were imaged using an EVOS FL cell imaging system (Invitrogen), and analyzed for differential fluorescence intensity per cell, using Fiji software.

Detection of Mitochondrial Membrane Potential with TMRM. Mitochondrial membrane potential (Ψm) was measured using tetramethylrhodamine methyl ester perchlorate (TMRM;

Thermo-Fisher Scientific, #T668) according to the manufacturer's protocol with some modifications. Briefly, cells were loaded with 200 nM dye in medium for 30 min at 37 ºC. The unfixed cells were then washed with PBS twice, immediately imaged with an EVOS FL cell imaging system, and analyzed for differential fluorescence intensity per cell using Fiji software.

Cellular Fractionation and Measurement of Cytosolic Mitochondrial (mt)DNA. Measurement of cytosolic mtDNA was based on a previously described method (16). Following exposure to αSyn monomers or oligomers, cellular fractionation was performed using a Mitochondria Isolation Kit for Cultured Cells (Thermo-Fisher Scientific, #89874) according to the manufacturer's instructions. DNA was then isolated from the cytosolic fraction using a Tissue DNA Kit (Biomiga, #GD2211-01) following the manufacturer's directions. Mitochondrial (mt)DNA encoding ND5, ND6 and COX1 were measured by quantitative real-time (qRT)PCR. Nuclear DNA encoding 18S ribosomal RNA was used for normalization. Human primer sequences were previously described (17).

Flow Cytometry. Cells were washed and detached in a non-enzymatic manner and incubated with Fc Receptor Blocking Solution (BioLegend, #422301) for 5 min at RT followed by staining with mouse anti- CD11b-APC (1:20; BioLegend #301310), rat anti-CSF1R APC (1:20, BioLegend, #347306), mouse anti-CD14 APC (1:5, BD Biosciences, #555399), and rat anti-CX_3CR1 PE (1:20, BioLegend #341603) for 30 min on ice. Cells were washed, and antigen expression was determined using cytoFLEX (Beckman Coulter), and analyzed with FlowJo V10.1 software (FlowJo, OR, USA).

qRT-PCR. Total RNA was extracted using a Quick-RNA™ MiniPrep kit (Zymo Research, # R1055), and each sample was reverse transcribed using a QuantiTect Reverse transcription kit (Qiagen, # 205313). qRT-PCR reaction was performed with LightCycler 480 SYBR Green I MasterMix (Roche) in a LightCycler480II instrument (Roche). The following primers were purchased from Qiagen: IL-6 (QT00083720); CD33 (QT00014672); IL-1β (QT00021385); TREM2 (QT00063868). All other primer sequences were designed using Primer Bank (18) and are listed in **Table S2.** Data were normalized to 18s rRNA expression, and analyzed with Prism 7.04 software (GraphPad).

Immunocytochemistry. EBs at various days of differentiation were allowed to attach to poly D-lysine (Sigma-Aldrich, P7280)-coated 24-well plates for 24 h. Cells, EBs or mouse brain sections were fixed with 4% PFA for 15 min, washed 3 times with PBS, and blocked with 3% BSA 0.3%

Triton X-100 in PBS for 30 min. Cells or sections were incubated with primary antibody in blocking solution overnight at 4°C, then washed with PBS, and the appropriate Alexa Fluor (488, 555, 647) conjugated secondary antibodies were used at 1:1,000, plus Hoechst 33342, Trihydrochloride, Trihydrate dye (1:1,000, Thermo-Fisher Scientific, # H3570) to visualize nuclei, for 1h at RT.

For microglia characterization, primary antibodies and dilutions were as follows: rabbit anti-Pu.1 (1:100; CST, #2266), goat anti-Iba1 (1:200; Abcam, #ab5076), rabbit anti-TMEM119 (1:200; Sigma, #HPA051870), rabbit anti-P2RY12 (1:100; Sigma, #HPA014518), mouse anti-CD41 (1:250; Abcam, #ab11024), rabbit anti-GYPA (CD235a, 1:200; Sigma, #HPA014811)**,** rabbit anti-VE-cadherin (1:400; CST, #2500), and rabbit anti-c-Kit (1:200; CST, #3074).

For co-culture experiments, primary antibodies and dilutions were as follows: rabbit anti-Iba1 (1:500; Abcam, #ab178680), mouse anti-Tubulin β3 (1:250, BioLegend, #801201), and mouse anti-human nuclear antigen (1:500, Abcam, #ab215396). Coverslips were mounted on slides with fluorescent mounting medium (DAKO) and visualized with a Zeiss Axiovert (100M) epifluorescence microscope.

For experiments studying hiMG engraftment into mouse brain, the following primary antibodies were used: Mouse anti-NeuN (1:250, Abcam, #ab104224), goat anti-Iba1 (1:200; Abcam, #ab5076), Rabbit anti-ASC (Adipogen, AG-25B-0006, 1:200), rabbit anti-cleaved caspase-3 (1:500, Cell Signaling, #9664), rabbit anti-caspase-1 (1:50, EMD Millipore, #AB1871), and mouse anti-Human Nuclear Antigen (HuNu, 1:500, Abcam, #ab191181). Imaging was performed using ImageXpress automated high-content confocal microscopy (Molecular Devices) or with an A1 confocal microscope (Nikon). All imaging conditions were identical for each set of stains (e.g. exposure time and laser power). Co-localization of cleaved/activated caspase-3 with $NeuN^+$ cells or cleaved/activated caspase-1 with Iba1 and Human Nuclear Antigen positive cells was measured using Fiji software. For co-localization of cleaved/activated caspase-3 with $NeuN^+$, masks were generated based on $NeuN^+$ staining, and the number of caspase-3 positive cells were counted and calculated as a percentage of total NeuN-positive cells. For co-localization of caspase-1 with Iba1 and HuNu, masks were generated based on Iba1 and HuNu double-positive cells, and then the intensity of caspase-1 was measured. For each mouse, at least 3 images were taken and averaged for analysis. All imaging and quantification were performed in a masked fashion, and under the same masking/thresholding settings.

Microglial Phagocytosis. hiMG were incubated with pHrodo® Red Zymosan Bioparticles® (Life Technologies, #P35364) at a concentration of 0.5 mg/ml for 2 h at 37 ^oC according to the manufacturer's specifications and as previously described (19). The cells were then fixed and

stained with anti-TMEM119 antibody and Hoechst 33342 dye to visualize cell nuclei. Phagocytosis was visualized by epifluorescence microscopy (Zeiss Axiovert 100M).

RNA-seq Data Acquisition and Mapping. RNA samples from hiMG, human fetal microglia (FMG; Clonexpress, #HMG030), hiPSC, and human neural progenitor cells (hNPC) were used for analysis (total of n = 8 samples). RNA was quality checked before sequencing by Qubit RNA Assay, RNA screenTape (Agilent tape station) and nanodrop. All RNA samples had an RNA integrity Number (RIN) >9. RNA libraries were prepared via poly A selection. Sequencing was performed on the Illumina HiSeq2500 platform in a 1x50 bp single end (SR) configuration in High Output mode (V4 chemistry) with ≥ 250 million reads per lane. Additional raw data for samples were downloaded from the Sequence Read Archive (ERP003613, SRP001371, SRP082406, SRP092075, SRP000996, and phs001373.v1.p1) as detailed in **Dataset S2*A***. When necessary, *.sra formatted data were converted to the *.fastq format using the SRA Toolkit (version 2.4.1). Data quality was assessed using FastQC (version 0.10.1) before being mapped to known Ensemble genes (GRCh37/NCBIM37) using Tophat2 (version 2.0.13). Raw read counts for each gene were obtained using Subread (version 1.4.2). All ftp data accessions and Tophat2/Subread mapping statistics are provided in **Dataset S2*A*.**

Bioinformatic Differential Expression Analysis of hiMG vs. other monocytoid cells. Raw read count data were read into R and combined into a single data frame for differential expression analyses using linear modeling strategies. Sample group annotations required for normalization and differential expression analyses are provided in **Dataset S1*B*.** The RNA-seq expression sets were filtered to include genes having cpm values ≥ 5 in 4 or more samples (n = 21,395). Raw read counts were normalized using the trimmed mean of M-values (TMM) method (20), and precision weights were calculated using voom (21) prior to differential analysis using the limma empirical Bayes analysis pipeline (22). Differential gene expression analyses were identified via a series of comparisons between sample groups specified by contrast matrices provided in the **Supplementary Materials ("*FINALcode.r*")**.

hiMG samples were first compared to hiPSC samples from three independent sources (total of n = 10 samples). The Benjamini and Hochberg procedure was used to calculate FDR-adjusted P-values for both differentially expressed genes. Genes were identified as significant at FDR-Q ≤ 0.01 and FC ≥ 2. To provide broader context for this analysis, we analyzed additional RNA-seq data obtained from primary brain microglia and 169 published samples from disparate primary cells, hiPSCs and their differentiated progeny (complete summary of annotations and mapping statistics provided in **Dataset S2)**. Hierarchical clustering of the 182 samples analyzed according to the 2,232 genes that were upregulated in hiMG parsed the samples into 2 primary clusters **(Fig. S2*A*).** One of the primary clusters was split into 2 distinct sub-clusters that were

comprised of all microglial samples (*n* = 84) or a mixture of all monocyte samples and myeloid dendritic samples **(Fig. S2*B-D*)**. These results demonstrate that the pattern of gene expression in hiMG is highly conserved among their brain-derived counterparts (23), microglia differentiated from hiPSCs using various protocols (24, 25), and to a lesser extent samples of closely-related cell types from the myeloid lineage (monocytes and dendritic cells). We confirmed these relationships in an unbiased manner by calculating all pair-wise Pearson correlations between the 182 samples according to the 10% most variable genes in the dataset (*n* = 2,140) to create a correlation matrix. Hierarchical clustering of the samples resulted in two primary groups that were identical to those observed in **Fig. S2*A*,** with the exception that adult lymph node and spleen samples were also parsed into a cluster comprised of the microglia and other myeloid lineage samples (cluster 2; **Fig. S2*A*)**.

Given the observed similarity in gene expression among microglial samples of diverse origin, we next set out to identify a set of 'microglial signature genes' with high levels of expression across microglial samples and low levels of expression in other cell types. To identify such genes, we separated the samples into three groups for comparison: Group 1 contained all samples comprising cluster 1 of the correlation matrix (red text, **Fig. S2*A*)**. Group 2 contained the non-microglial samples from cluster 2 of the correlation matrix (green text, **Fig. S2*A*)**, and Group 3 included all microglial samples from cluster 2 (blue text, **Fig. S2*A*)**. Genes were then classified as part of the microglial signature if they met the following four criteria: (1) significantly higher expression (FDR ≤ 0.01, fold change ≥ 2) in Group 3 vs. Group 1, (2) significantly higher expression in Group 3 vs. Group 2, (3) mean-centered counts per million (cpm) expression values > 0 in at least 90% of Group 3 samples, and (4) mean-centered cpm expression values < 0 in at least 90% of Group 2 samples. This classification scheme produced a microglial signature comprised of 53 genes **(Fig. S2*B* and Dataset S3)**, including several previously linked to microglia such as Triggering Receptor Expressed on Myeloid Cells 2 (*TREM2*) (26, 27), Scavenger receptor B1 (*SCARB1)(28)*, and complement C3 (29, 30). Moreover, we uncovered additional genes associated with the microglial phenotype, such as oxidized low-density lipoprotein receptor 1 (*OLR1*), which were shown to promote synaptic pruning, and deafness associated tumor suppressor (DFNA5), whose function remains poorly defined.

Bioinformatic Analysis for Functional Enrichment. All functional enrichments were performed with the Genomic Regions Enrichment of Annotations Tool (GREAT) (31) using Ensemble genes (GRCh37/NCBIM37) genome coordinates. The initial set of 21,395 genes with detectable expression was used as 'Background Regions,' and the 'Association Rule' was set to 'single nearest gene' excluding curated regulatory domains.

Statistical Analysis. Data comparisons were carried out using an analysis of variance (ANOVA) analysis with Bonferroni post-hoc test. Data with *P*-values < 0.05 were considered statistically significant. Comparison of samples were performed in a masked fashion.

Data Availability. The data that support the findings of this study are available from the corresponding author upon reasonable request.

Code Availability. Source code used to generate results that are reported in the paper is available as **"*FINALcode.r*"**.

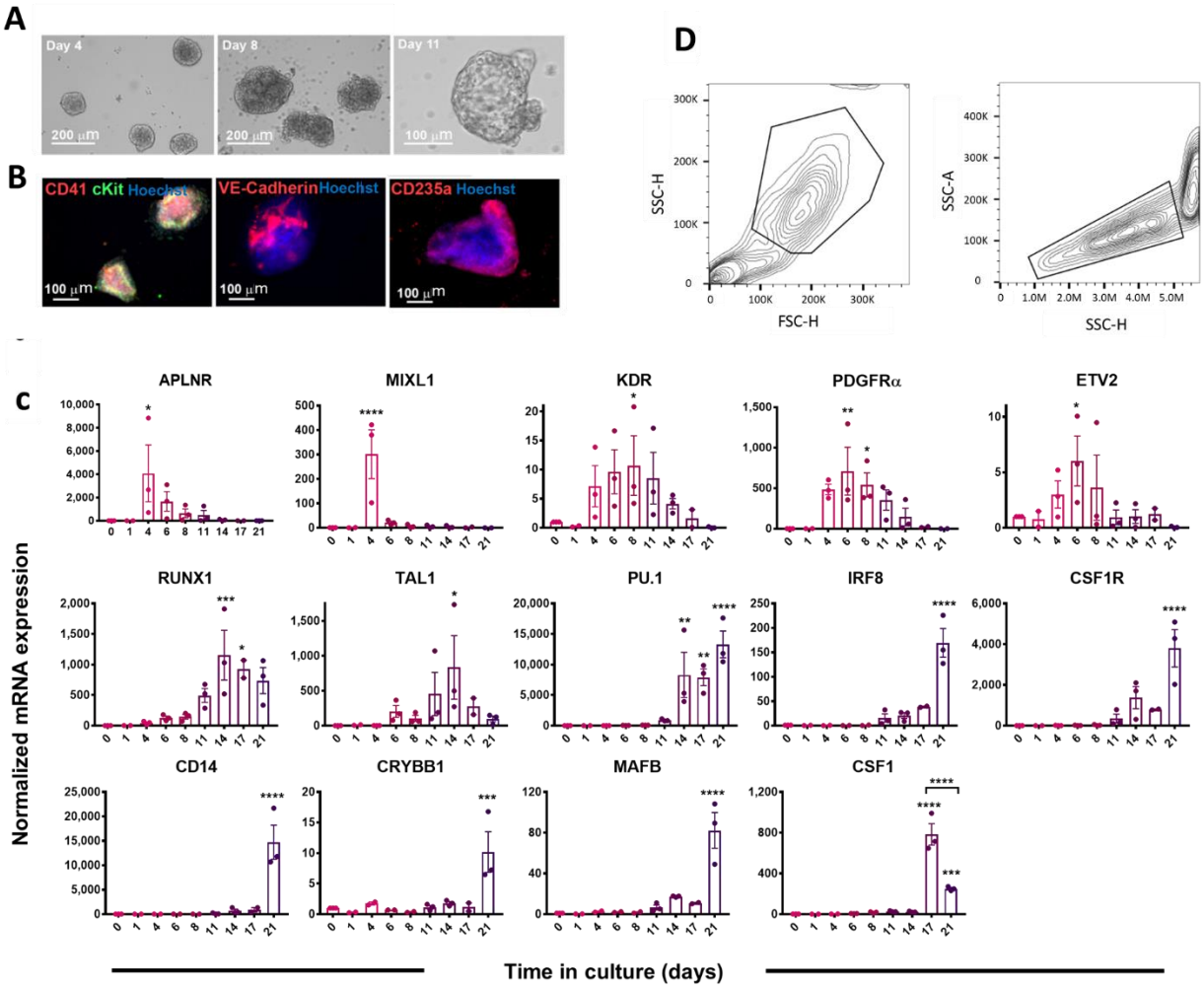

Fig. S1. Differentiation of human iPSCs into microglia-Like cells (hiMG). *(A)* Representative bright-field images of differentiating embryoid bodies (EBs) at day 4, 8 and 11 of differentiation. *(B)* Representative immunofluorescent images of day 4 EBs, showing CD41, cKit, VE-Cadherin and CD235a. *(C)* Expression levels of key differentiation genes at days 0-21 of differentiation (*n* =3 independent biological replicates). Graphs indicate mean + SEM. Statistical analysis performed using a two-way ANOVA with Bonferroni post-hoc test (**P* < 0.05; ***P* < 0.01; ****P* < 0.001; *****P* < 0.0001 compared to day 0 unless otherwise stated). *(D)* Gating strategy for flow cytometry analysis based on side scatter height (SSC-H) vs. forward scatter height (FSC-H) for debris exclusion and side scatter area (SSC-A) vs. side scatter height (SSC-H) for doublet exclusion.

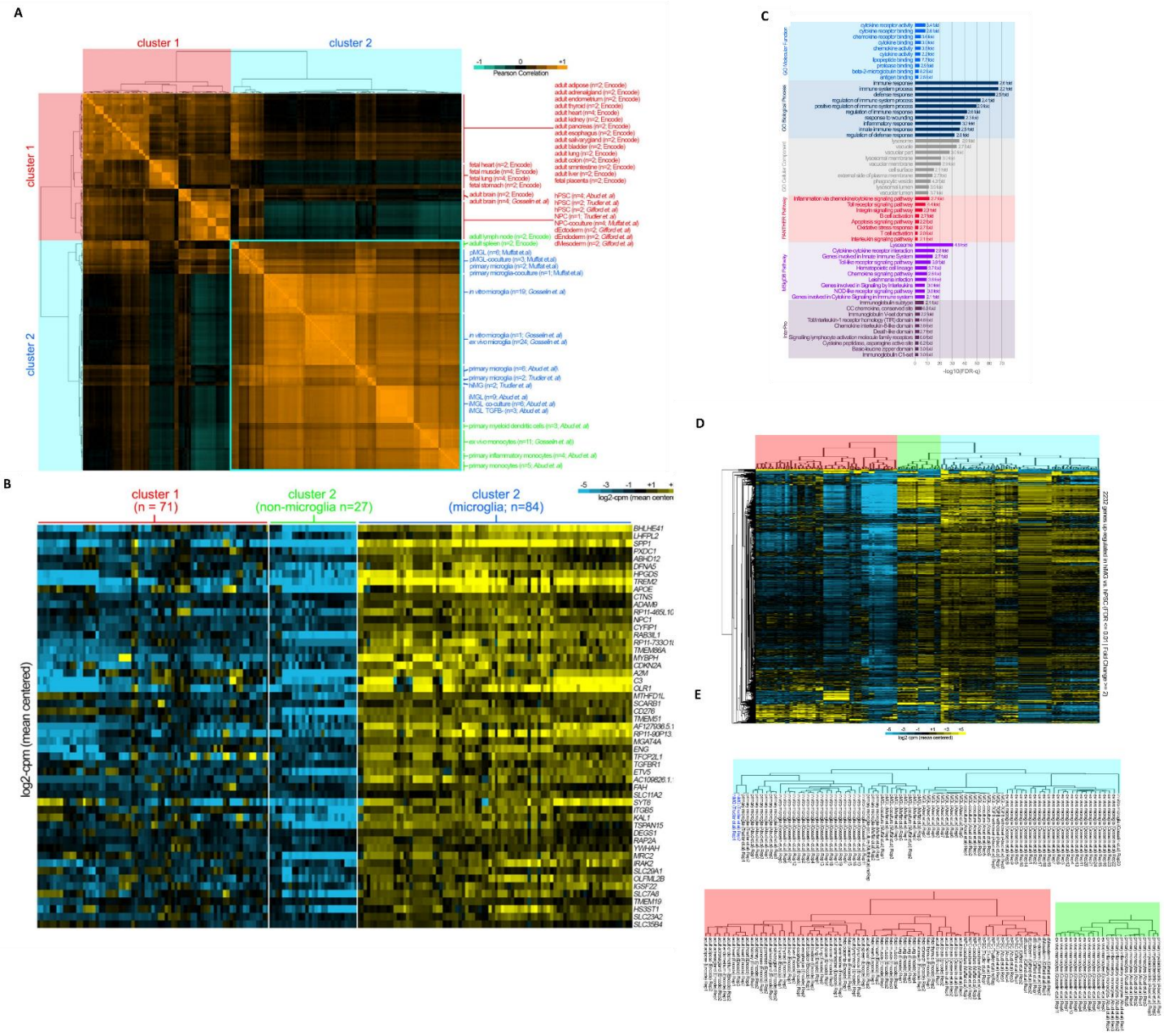

Fig. S2. Transcriptional characterization of hiMG. (*A*) transcriptional signature is consistent with reported human microglia transcriptomes. Human RNA-seq data from *ex vivo* microglia, *in vitro* microglia, primary microglia, *ex vivo* monocytes, primary monocytes, primary myeloid dendritic cells, 17 distinct adult human tissues, 6 fetal tissues, hiPSC samples, and non-microglia hiPSC differentiations. Clustering of samples according to Pearson correlation values between all 182 samples in the analysis. Pearson Correlations were calculated according to the 10% most variable detected genes (*n* = 2,140). Samples were clustered using Euclidean distance with average linkage. Cluster 1 (red text), contains all non-immune samples; Cluster 2 contains all immune cells, which includes non-microglia samples (green text) and microglia (blue text). (n shown in parenthesis, and in detail in **Dataset S2*A***). *(B)* Heatmap depicting gene expression values (mean centered log-cpm) for microglial signature genes (*n* = 53). The criteria for defining signature genes are described in the methods. The sample groups shown at the top of the heatmap are color coded to match the sample descriptions to the right of the correlation clustering heatmap in panel a. Group membership for each sample is provided in column labeled

"*Microglial_Signature_Group*" of **Dataset S2*B***. *(C)* Functional enrichment results for genes with elevated expression in hiMG relative to undifferentiated hiPSCs. GREAT was used to assess functional enrichment for the 2,232 genes with significantly higher expression in hiMG (FDR-Q ≤ 0.01 and FC ≥ 2) compared to hiPSC, which are provided in **Dataset S1*A***. No more than the 10 most significant terms for each ontology set are provided. Within each ontology set, the terms are sorted according to significance (-log10(FDR-q)) and fold enrichment (observed/expected). Detailed results, including the underlying genes driving the functional enrichments, are provided in **Dataset S1*B***. *(D)* Hierarchical clustering of all 182 samples in the analysis. Clustering according to the 2,232 genes with significantly higher expression (FDR-Q ≤ 0.01 and FC ≥ 2) in hiMG compared to hiPSC, as provided in **Dataset S1*A***. Samples were clustered using Euclidean distance with average linkage. Samples are labeled as non-immune (red); non-microglial immune (green); microglia (blue). *(E)* Samples within each color-coded branch of the dendrogram in panel D are expanded.

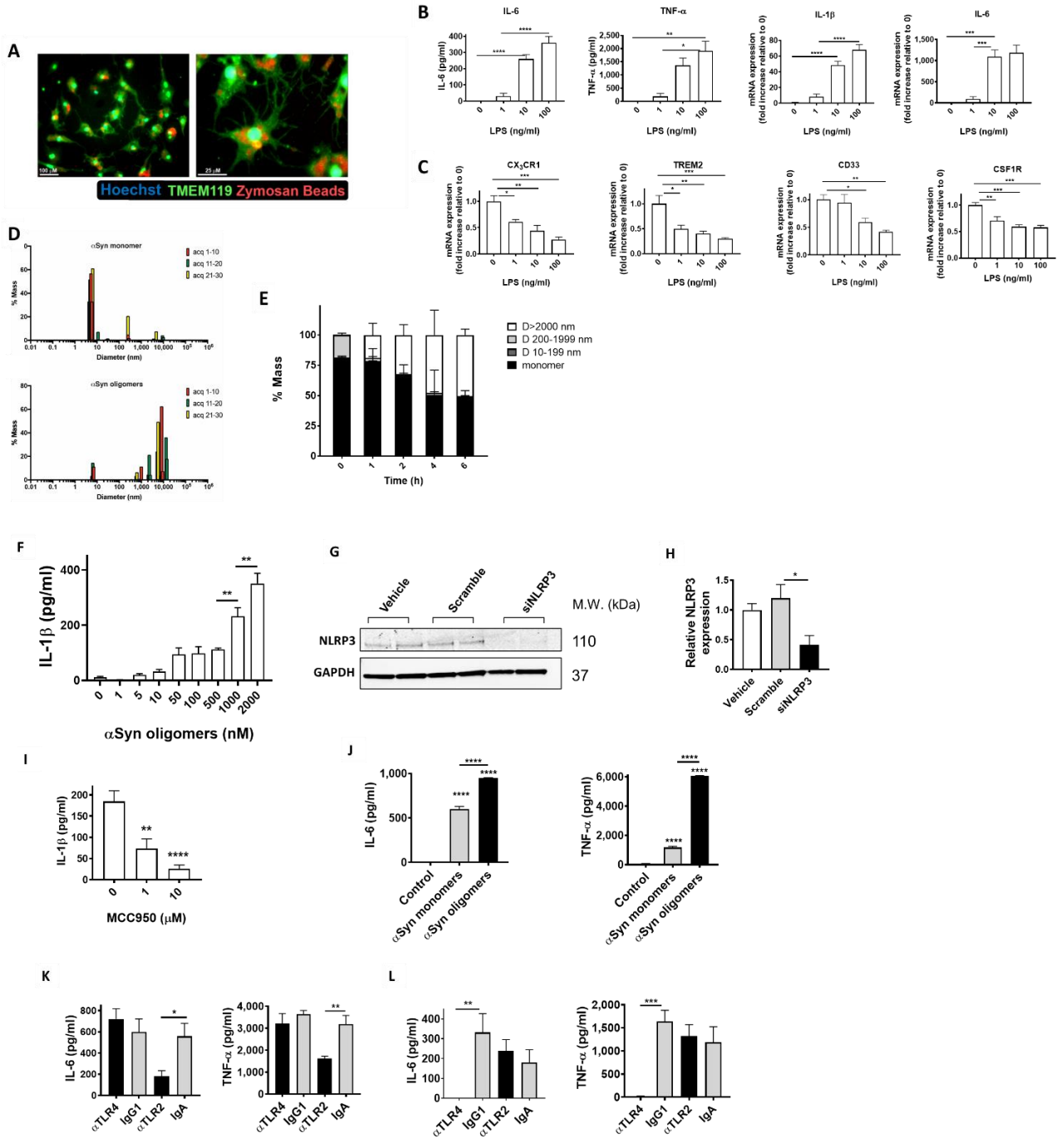

Fig. S3. Oligomeric αSyn Induces NLRP3 Inflammasome and Pro-Inflammatory Response in hiMG via TLR2. *(A)* Representative images of zymosan-pHrodo bioparticles (red), TMEM119 (green) and Hoechst (blue). *Left:* low magnification (scale bar, 100 µm). *Right:* higher magnification (scale bar, 25 µm) showing zymosan particles in cells. *(B)* Functional analysis of LPS-stimulated hiMG. Dose-dependent increase in cytokine secretion of IL-6 and TNF by ELISA and mRNA levels of IL-1β and IL-6 by qRT-PCR (n =3-6). *(C)* Measurement of LPS dose-dependent mRNA expression of CX_3CR1, TREM2, CD33 and CSF1R (n = 4-5). *(D)* Dynamic light scattering (DLS) reveals predominantly monomeric αSyn (diameter <10 nm) in monomer

preparations (*top*), in contrast to largely aggregated αSyn in oligomer preparations (*bottom*). Three sets of ten acquisitions (acq) each of representative samples are shown as % mass and apparent hydrodynamic diameter. *(E)* DLS was used to assess the presence of αSyn aggregates at specific time-points over 6 h. Particles detected by DLS were categorized into monomers (black bars), and aggregates of increasing hydrodynamic diameter (D) ranging from 10-200 nm (dark grey), 200-2,000 nm (light grey) and large aggregates >2000 nm (white). Three sets of ten acquisitions each of representative samples are shown as % mass and apparent hydrodynamic diameter (D). *(F)* Dose-response effect of oligomeric αSyn on IL-1β secretion from hiMG (*n* = 4-6). *(G)* Representative blot of NLRP3 protein levels following treatment with siRNA. *(H)* Quantification of NLRP3 protein expression following siRNA relative to vehicle (n = 3-4). *(I)* Dose effect of NLRP3 inhibitor MCC950 on IL-1β secretion following oligomeric αSyn (750 nM, *n* = 6-8). *(J)* Oligomeric αSyn (750 nM) increases IL-6 and TNF secretion compared to monomers (*n* = 3-5). *(K)* Neutralizing antibody against TLR2 blocks oligomeric αSyn-induced IL-6 and TNF release (*n* = 5-7). *(L)* Neutralizing antibody against TLR4 blocks LPS-induced IL-6 and TNF release (*n* = 3-6). Graphs indicate mean + SEM. Statistical analysis performed using a two-way ANOVA with Bonferroni post-hoc test (**P* < 0.05; ***P* < 0.01; ****P* < 0.001; *****P* < 0.0001 compared to control unless otherwise stated).

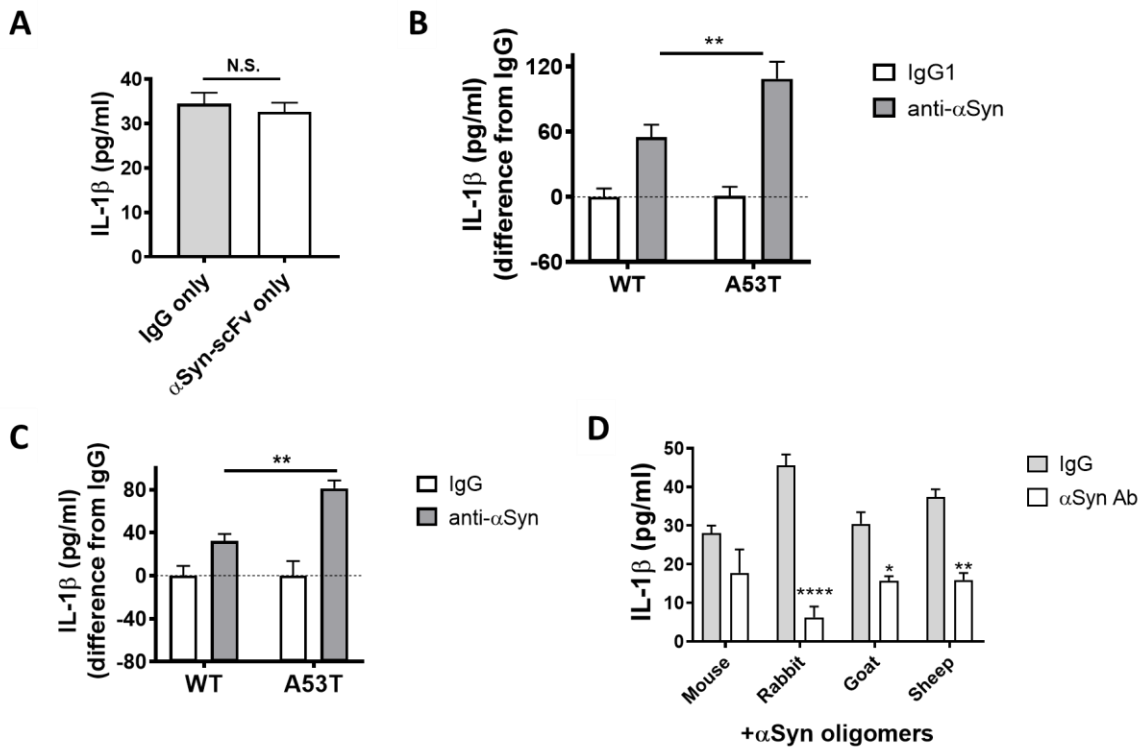

Fig. S4. Mouse and Rabbit αSyn Antibodies Exacerbate Inflammasome Activation and IL-1β Release from hiMG. *(A)* IL-1β release from hiMG incubated with humanized αSyn scFv or human IgG1 control only, showing no immune activation (n = 5/group). (*B*) IL-1β secretion from hiMG exposed to CM from gene-corrected WT and A53T DA neurons pre-treated with mouse anti-αSyn Ab compared to isotype IgG1 control (n = 10-12). *(C)* IL-1β release from hiMG exposed to CM from gene-corrected WT or A53T DA neurons pre-treated with rabbit anti-αSyn Ab compared to isotype IgG controls (*n* = 5-6). *(D)* IL-1β release from primary mouse microglia, incubated with oligomeric αSyn (750 nM oligomers by DLS) pre-treated with antibodies against αSyn generated in various species (n = 4-6). Graphs indicate mean + SEM. Statistical analysis performed using a two-way ANOVA with Bonferroni post-hoc test (***P* < 0.01; *** *P* < 0.001. N.S., not significant (*P* = 0.59).

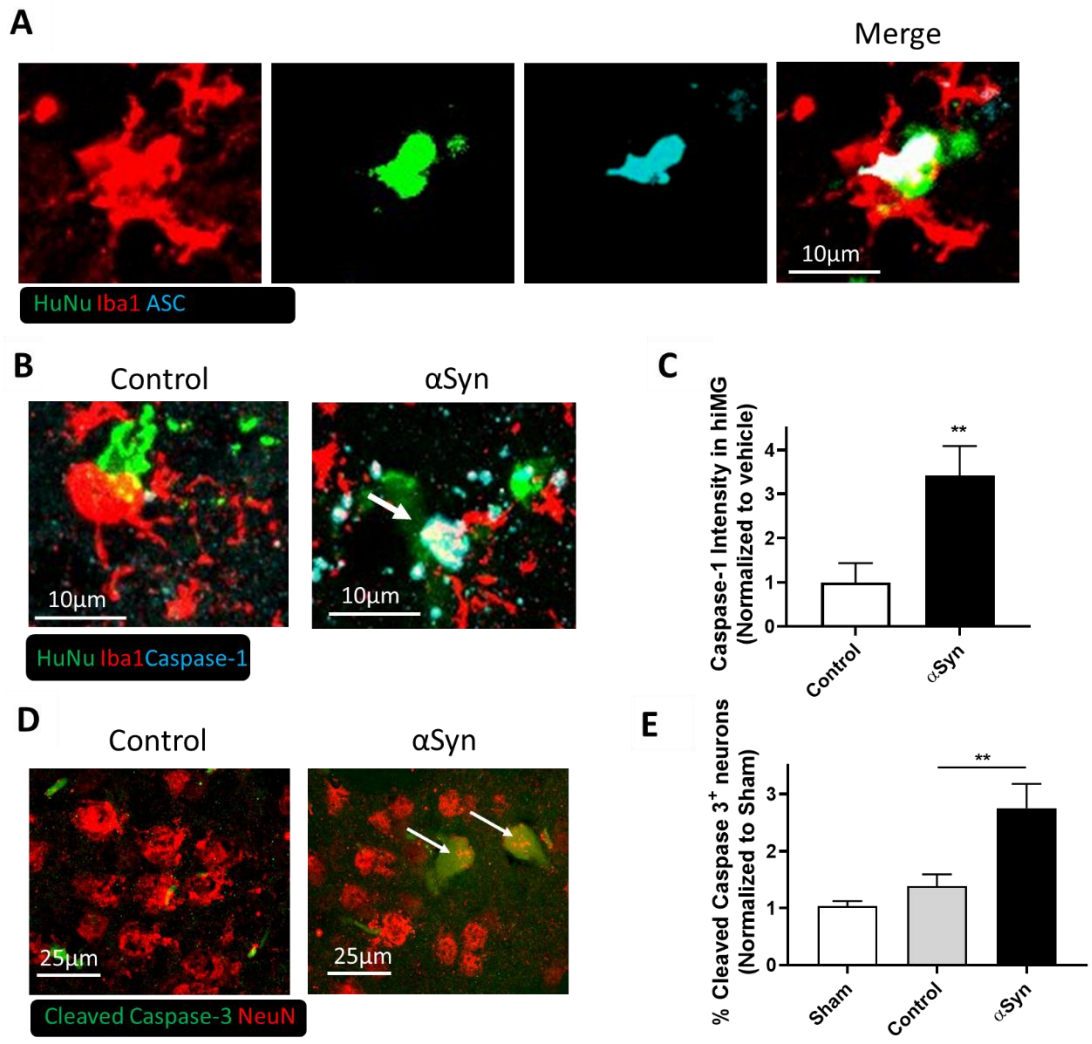

Fig. S5. αSyn Pre-Treatment Activates the Inflammasome and Induces Neuronal Death in hiMG-Engrafted Mice. *(A)* Representative image showing ASC specks in transplanted hiMG. Human nuclei antigen (HuNu; green), Iba1 (red) and ASC (cyan). Scale bar, 10 µm. *(B)* Representative images showing cleaved/activated caspase-1 staining (arrow) in transplanted hiMG after αSyn exposure (*right*) but not in control (*left*). Human nuclei antigen (HuNu; green), Iba1 (red) and activated caspase-1 (cyan). Scale bar, 10 µm. *(C)* Quantification of the caspase-1 intensity in engrafted hiMG ($Iba1^{+}HuNu^{+}$ cells) (*n* = 9-11). *(D)* Representative images of cleaved/activated caspase-3 staining in endogenous mouse neurons after transplantation of control (*left*) or αSyn-activated hiMG (*right*). Cleaved caspase-3 (green, indicated by arrows) and NeuN (red). Scale bar, 25 µm. *(E)* Quantification of cleaved caspase-3 in neurons ($NeuN^{+}$ cells) (*n* = 6-7). Graphs indicate mean + SEM. Statistical analysis performed using a two-way ANOVA with Bonferroni post-hoc test (***P* < 0.01).

Base media	Growth factors	Cat No.
<u>hiMG induction medium (MGIM):</u> StemPro34 (Gibco, #10639011) + GlutaMAX (2 mM; GIbco, #35050061) L-ascorbic acid 2-phospate (64 µg/ml; Sigma-Aldrich, # A8960) 1-Thioglycerol (0.46 mM; Sigma-Aldrich, # M1753)	10 ng/ml BMP4 10 µM Y27632	R&D systems, #314-BP STEMCELL Technologies, #72302
	10 ng/ml BMP4 1µM Y27632 10 ng/ml FGF2	R&D systems, #314-BP STEMCELL Technologies, #72302 R&D systems, #4114-TC-01M
	1 ng/ml FGF2 10 ng/ml VEGF 10 ng/ml I-L6 40 ng/ml IL-3 100 ng/ml SCF	R&D systems, #4114-TC-01M R&D systems, #293-VE-050/CF Peprotech, #200-06-B R&D systems, #203-IL-050/CF Thermo-Fisher, #PHC2111
	10 ng/ml VEGF 10 ng/ml IL-6 40 ng/ml IL-3 50 ng/ml TPO 100 ng/ml SCF	R&D systems, #293-VE-050/CF Peprotech, #200-06-B R&D systems, #203-IL-050/CF Thermo-Fisher, #PHC9514 Thermo-Fisher, #PHC2111
<u>hiMG differentiation medium:</u> IMDM (Gibco, #12440053) + N2 (1%, Gibco, #17502048) Bovine Albumin Fraction V (0.5% v/v, Gibco, #15260037) AlbuMAX (0.2% w/v, Gibco, # 11020039) Sodium Pyruvate (1% v/v, Gibco, #11360070) L-ascorbic acid 2-phospate (64 µg/ml)	100 ng/ml IL-34 10 ng/ml GM-CSF	Peprotech, #200-34 R&D systems, #215-GM-050/CF

Table S1. Detailed information about media composition, growth factors and catalog numbers for microglial differentiation.

Gene	Forward	Reverse
18S	GTCGTAGTTCCGACCATA	GCCCTTCCGTCAATTCCTTT
APLNR	CTCTGGACCGTGTTTCGGAG	GGTACGTGTAGGTAGCCCACA
CD14	ACGCCAGAACCTTGTGAGC	GCATGGATCTCCACCTCTACTG
Crybb1	GTGCTCAAATCTGGCAGACC	GGAAGTTGGACTGCTCAAAGG
Csf1	TGGCGAGCAGGAGTATCAC	AGGTCTCCATCTGACTGTCAAT
CSF1R	GGGAATCCCAGTGATAGAGCC	TTGGAAGGTAGCGTTGTTGGT
ER71	GAAGGAGCCAAATTAGGCTTCT	GAGCTTGTACCTTTCCAGCAT
Irf8	ATGTGTGACCGGAATGGTGG	AGTCCTGGATACATGCTACTGTC
KDR	GGCCCAATAATCAGAGTGGCA	CCAGTGTCATTTCCGATCACTTT
MAFB	TCAAGTTCGACGTGAAGAAGG	GTTCATCTGCTGGTAGTTGCT
MIXL1	GGCGTCAGAGTGGGAAATCC	GGCAGGCAGTTCACATCTACC
PDGFRa	TGGCAGTACCCCATGTCTGAA	CCAAGACCGTCACAAAAAGGC
PU.1	GTGCCCTATGACACGGATCTA	AGTCCCAGTAATGGTCGCTAT
RunX1	CTGCCCATCGCTTTCAAGGT	GCCGAGTAGTTTTCATCATTGCC
TAL1	AGCCGGATGCCTTCCCTAT	GGGACCATCAGTAATCTCCATCT

Table S2. List of sequences of primers that were used for qRT-PCR analysis.

Dataset S1 (separate file). Differential Gene Expression in hiPSCs and Differentiated hiMGs. *(A)* Statistics from analysis of differential expression between hiPSCs and hiMGs. *(B)* Detailed results from the analysis of functional enrichment of genes with elevated expression in hiMG relative to undifferentiated hiPSCs.

Dataset S2 (separate file). Published RNA-seq Data vs. RNA-seq Data of hiMG in this Study. RNA-seq data of an additional 169 samples from unrelated hiPSCs, non-microglia hiPSC differentiations (hNPCs; dEctoderm; dEndoderm; dMesoderm), microglia derived from hiPSCs using distinct protocols (pMGL; iMGL), *ex vivo* microglia, in vitro microglia, primary microglia, *ex vivo* monocytes, primary monocytes, primary myeloid dendritic cells, 17 distinct adult human tissues, and 6 distinct fetal tissues. *(A)* Mapping statistics and data accessions for all 182 RNA-seq samples included in the study. *(B)* Sample annotations and sample groupings pertaining to differential expression analyses.

Dataset S3 (separate file). Materials Relevant to the Microglia Signature. *(A)* Statistics for the 2,164 genes with significantly elevated expression in Group 1 ("cluster 2 microglia" from **Fig. S2*B***) vs. Group 2 ("cluster 1" from **Fig. S2*B***). *(B)* Statistics for the 1,745 genes with significantly elevated expression in Group 1 ("cluster 2 microglia" from **S2*B***) vs. Group 3 ("cluster 2 non-microglia" from **S2*B***). *(C)* Summary of the final microglia signature genes depicted in **Fig. S2*B***.

1. K. Okita *et al.*, A more efficient method to generate integration-free human iPS cells. *Nat. Methods* **8**, 409-412 (2011).
2. M. Talantova *et al.*, Aβ induces astrocytic glutamate release, extrasynaptic NMDA receptor activation, and synaptic loss. *Proc. Natl. Acad. Sci. U.S.A.* **110**, E2518-E2527 (2013).
3. T. Lin *et al.*, A chemical platform for improved induction of human iPSCs. *Nat. Methods* **6**, 805-808 (2009).
4. H. T. Liu, B. A. Tashmukhamedov, H. Inoue, Y. Okada, R. Z. Sabirov, Roles of two types of anion channels in glutamate release from mouse astrocytes under ischemic or osmotic stress. *Glia* **54**, 343-357 (2006).
5. S. Kriks *et al.*, Dopamine neurons derived from human ES cells efficiently engraft in animal models of Parkinson's disease. *Nature* **480**, 547-551 (2011).
6. S. D. Ryan *et al.*, Isogenic human iPSC Parkinson's model shows nitrosative stress-induced dysfunction in MEF2-PGC1α transcription. *Cell* **155**, 1351-1364 (2013).
7. M. Wunderlich *et al.*, AML xenograft efficiency is significantly improved in NOD/SCID-IL2Rγ mice constitutively expressing human SCF, GM-CSF and IL-3. *Leukemia* **24**, 1785-1788 (2010).
8. F. Notta, S. Doulatov, J. E. Dick, Engraftment of human hematopoietic stem cells is more efficient in female NOD/SCID/IL-2Rγc-null recipients. *Blood* **115**, 3704-3707 (2010).

9. J. Saura, J. M. Tusell, J. Serratosa, High-yield isolation of murine microglia by mild trypsinization. *Glia* **44**, 183-189 (2003).
10. S. Emadi *et al.*, Inhibiting aggregation of α-synuclein with human single chain antibody fragments. *Biochemistry* **43**, 2871-2878 (2004).
11. S. Emadi, H. Barkhordarian, M. S. Wang, P. Schulz, M. R. Sierks, Isolation of a human single chain antibody fragment against oligomeric α-synuclein that inhibits aggregation and prevents α-synuclein-induced toxicity. *J. Mol. Biol.* **368**, 1132-1144 (2007).
12. Y. Levites *et al.*, Intracranial adeno-associated virus-mediated delivery of anti-pan Aβ, Aβ40, and Aβ42 single-chain variable fragments attenuates plaque pathology in amyloid precursor protein mice. *J. Neurosci.* **26**, 11923-11928 (2006).
13. D. Trudler *et al.*, α-Synuclein Oligomers Induce Glutamate Release from Astrocytes and Excessive Extrasynaptic NMDAR Activity in Neurons, Thus Contributing to Synapse Loss. *J. Neurosci.* **41**, 2264-2273 (2021).
14. P. Thakur *et al.*, Modeling Parkinson's disease pathology by combination of fibril seeds and α-synuclein overexpression in the rat brain. *Proc. Natl. Acad. Sci. U.S.A.* **114**, E8284-E8293 (2017).
15. J. Schindelin *et al.*, Fiji: an open-source platform for biological-image analysis. *Nat. Methods* **9**, 676-682 (2012).
16. K. Nakahira *et al.*, Autophagy proteins regulate innate immune responses by inhibiting the release of mitochondrial DNA mediated by the NALP3 inflammasome. *Nat. Immunol.* **12**, 222-230 (2011).
17. W. Wang *et al.*, The inhibition of TDP-43 mitochondrial localization blocks its neuronal toxicity. *Nat. Med.* **22**, 869-878 (2016).
18. A. Spandidos, X. Wang, H. Wang, B. Seed, PrimerBank: a resource of human and mouse PCR primer pairs for gene expression detection and quantification. *Nucleic Acids Res.* **38**, D792-799 (2010).
19. D. Trudler, O. Weinreb, S. A. Mandel, M. B. Youdim, D. Frenkel, DJ-1 deficiency triggers microglia sensitivity to dopamine toward a pro-inflammatory phenotype that is attenuated by rasagiline. *J. Neurochem.* **129**, 434-447 (2014).
20. M. D. Robinson, A. Oshlack, A scaling normalization method for differential expression analysis of RNA-seq data. *Genome Biol.* **11**, R25 (2010).
21. C. W. Law, Y. Chen, W. Shi, G. K. Smyth, voom: Precision weights unlock linear model analysis tools for RNA-seq read counts. *Genome Biol.* **15**, R29 (2014).
22. G. K. Smyth, Linear models and empirical bayes methods for assessing differential expression in microarray experiments. *Stat. Appl. Genet. Mol. Biol.* **3**, Article3 (2004).
23. D. Gosselin *et al.*, An environment-dependent transcriptional network specifies human microglia identity. *Science* **356** (2017).
24. E. M. Abud *et al.*, iPSC-Derived Human Microglia-like Cells to Study Neurological Diseases. *Neuron* **94**, 278-293 e279 (2017).
25. J. Muffat *et al.*, Efficient derivation of microglia-like cells from human pluripotent stem cells. *Nat. Med.* **22**, 1358-1367 (2016).
26. S. Krasemann *et al.*, The TREM2-APOE Pathway Drives the Transcriptional Phenotype of Dysfunctional Microglia in Neurodegenerative Diseases. *Immunity* **47**, 566-581 e569 (2017).
27. H. Keren-Shaul *et al.*, A Unique Microglia Type Associated with Restricting Development of Alzheimer's Disease. *Cell* **169**, 1276-1290 e1217 (2017).
28. S. E. Hickman *et al.*, The microglial sensome revealed by direct RNA sequencing. *Nat. Neurosci.* **16**, 1896-1905 (2013).

29. T. R. Hammond, S. E. Marsh, B. Stevens, Immune Signaling in Neurodegeneration. *Immunity* **50**, 955-974 (2019).
30. B. Stevens *et al.*, The classical complement cascade mediates CNS synapse elimination. *Cell* **131**, 1164-1178 (2007).
31. C. Y. McLean *et al.*, GREAT improves functional interpretation of cis-regulatory regions. *Nat. Biotechnol.* **28**, 495-501 (2010).